Topical Review

Quantitative functional analysis of protein complexes on surfaces

Hye Jin Lee[3], Yuling Yan[2], Gerard Marriott[1] and Robert M. Corn[3]

[1] *Department of Physiology, University of Wisconsin–Madison, WI, USA*
[2] *Department of Mechanical Engineering, University of Hawai'i Manoa, HI, USA*
[3] *Department of Chemistry, University of California–Irvine, CA, USA*

A major challenge in cell and molecular physiology research is to understand the mechanisms of biological processes in terms of the interactions, activities and regulation of the underlying proteins. Functional and mechanistic analyses of the large number of proteins that participate in the regulation of cellular processes will require new approaches and techniques for high throughput and multiplexed functional analyses of protein interactions, protein conformational dynamics and protein activity. In this review we focus on the development and application of proteomics and associated technologies for quantitative functional analysis of proteins and their complexes that include: (1) the application of surface plasmon resonance (SPR) imaging for multiplexed, label-free analyses of protein interactions, binding constants for biomolecular interactions and protein activities; and (2) high content analysis of protein motions within functional multiprotein complexes.

(Received 13 December 2004; accepted 16 December 2004; first published online 21 December 2004)
Corresponding author G. Marriott: Department of Physiology, University of Wisconsin, 1300 University Ave., Madison, WI 53706, USA. Email: gm@physiology.wisc.edu

Introduction

It has been argued that an understanding of the mechanisms that control cellular processes requires an appreciation of how the activities and interactions of proteins and their complexes are regulated and integrated in time and space (Roy *et al.* 2001; Pjizicky *et al.* 2003; Ping, 2003). This is a daunting task given the large number of potential protein interactions that exist in a cell – for example, scores of actin binding proteins are implicated in the regulation of cell motility (Pollard & Borisy, 2003) – and the finding that the activity and interactions of many proteins are regulated at specific sites and times in the cell (Choidas *et al.* 1998; Murakoshi *et al.* 2004). In principle complex cellular processes such as motility can be studied through a global analysis of gene expression, which may reveal specific genes whose expression is coupled to the perturbation. However, the correlation between the level of a specific mRNA and the corresponding protein is not strong (Gygi *et al.* 1999) and, furthermore, gene expression profiles are largely blind to the post-translational protein modifications that underlie the regulation of many cellular processes.

A more complete understanding of the regulation of cell function and behaviour may be better served by studying the interactions and functions of the underlying proteins (Zhu *et al.* 2001). Functional proteomics is a rapidly developing field that borrows concepts and methodologies from biology, chemistry, physics and engineering to understand biological function in terms of the activities and interactions of the underlying proteins. Many of the functional proteomic studies described to date are qualitative and discovery based and seek to merely identify the proteins within complexes. However, there is also a need for more quantitative analysis of functional proteomics that can elucidate the mechanisms that regulate the formation and activities of specific protein complexes. Given the fantastic number of potential protein complexes that exist within a cell, there is a tremendous need to develop (1) new technologies and platforms for high throughput, multiplexed and quantitative analyses of protein interactions and activities, and (2) high-content analyses of protein complexes that elucidate the mechanisms underlying their function. These studies should include a quantitative analysis of functional motions or reactions that lead to a specific activity or regulation of the protein complex.

Recent studies demonstrate that engineered surfaces harbouring microarrays of functional proteins (protein chips; Zhu *et al.* 2000, 2001; MacBeath & Schreiber, 2000; Chen *et al.* 2003) can be used for massively parallel, multiplexed kinetic and thermodynamic analyses

 DOI: 10.1113/jphysiol.2004.081117

of protein interactions and protein activity. In this review, we focus on two specific approaches for the quantitative analysis of protein interactions and function: (i) the multiplexed SPR imaging (label-free) analysis of enzymatic activity and the determination of the association and dissociation rates for protein complexation, and (ii) the high content fluorescence based analysis of protein motions within functional multiprotein complexes. The reader can find the following reviews on the applications of mass spectrophotometry to proteomics: Resing (2002), Aebersold & Mann (2003) and Graves & Haystead (2003); while key concepts and methodologies used in functional proteomics have recently been reviewed by Ping (2003) and Zhu & Snyder (2003).

Thermodynamics of protein complex formation

Given the finite lifetime of protein complexes, high throughput analysis of protein interactions on protein chips should be performed using a concentration of target protein that significantly exceeds the dissociation constant for the capture-target protein complex. This condition is rarely met for fluorescence detection of surface bound target because the chip is washed to remove unbound detection probes – this action reduces the concentration of target protein to well below the equilibrium constant and so the amount of protein complex bound to a surface after a given period of time will be governed by the rate of complex dissociation. Clearly, then, sensible measurements of protein complexes using fluorescence detection require that the period between the dilution and detection events is far shorter than the time constant for complex dissociation. How long can this period be? For a protein complex having a equilibrium dissociation constant of 10^{-8} M that is formed with a bimolecular rate constant of 10^{7} M^{-1} s^{-1}, the rate of complex dissociation will be 0.1 s^{-1} or a time constant of 10 s. Thus any protein subunit that is weakly bound within a surface bound complex will rapidly dissociate under this condition and only a vanishingly small percentage will remain for functional analyses. The thermodynamics of protein interactions thereby sets a strict limit on the types of complexes that can be studied using protein microarrays and fluorescence detection – this limitation particularly affects the functional proteomic analysis of rapid cellular processes such as exocytosis and cell motility, which are necessarily regulated by short lived protein interactions. On the other hand, strongly bound protein complexes, e.g. a surface-bound capture antibody-target protein, will usually exhibit an equilibrium dissociation constant of 10^{-12} M, which with a bimolecular rate constant of 10^{7} M^{-1} s^{-1} will persist for an average lifetime of nearly 28 h. Consequently, multiplexed, fluorescence based detection of protein complexes on protein chips are usually limited to monomeric proteins that are covalently or tightly bound to the surface or to extremely stable protein complexes.

Surface based, functional analyses of protein interactions, protein activities and conformational dynamics

Fluorescence based detection of protein interactions. Fluorescence spectroscopy and fluorescence imaging techniques are routinely used to quantify the activity, interactions and dynamics of proteins even to the level of single molecules (Kron & Spudich, 1986). Furthermore, fluorescence detection is suitable for quantifying protein binding reactions and protein content over a very large dynamic concentration range. In practice, a captured target protein is usually detected on the chip surface by using a biotinylated monoclonal antibody that recognizes a separate epitope on the target protein. The detection antibody is tagged by using a fluorescently labelled streptavidin – alternatively, the detection antibody can be tagged with fluorescently labelled second antibodies raised against the detection antibody. The level of background signal that arises primarily from the non-specific binding of fluorescent detection reagent to the chip surface dictates the sensitivity of the fluorescence readout. The magnitude of the background signal depends on the nature of the optical probe and the protein to which it is attached.

Label free detection of protein interactions and activities. Label free detection of protein interactions, on the other hand, can be made without exchanging the biological sample since the measurement is based on a change in a surface property as described below. Quantitative measurements of multiple protein association reactions, such as the rate of complex formation, can therefore be performed directly in the biological sample, e.g. a cell lysate or serum. Furthermore by exchanging the biological sample with buffer, it is also possible to use the same protein chip to determine the rate of complex dissociation.

Multiplexed analysis of protein interactions using surface plasmon resonance (SPR). SPR is a surface sensitive optical technique that can be powerfully applied to study bioaffinity interactions in a label-free manner on gold or noble metal thin films. SPR is based upon the creation of surface plasmons (SPs), which are oscillations of free electrons that propagate parallel to a metal/dielectric interface. In order to excite SPs, p-polarized light is reflected through a particular optical geometry typically involving a prism–noble metal film–dielectric layer assembly (Homola *et al.* 1999). The SPs are evanescent waves that have a maximum charge density at the interface and decay exponentially from the surface of the metal with

a typical decay length of about 200 nm. Within this region, SPR is sensitive to any changes in the index of refraction caused by adsorption of molecules onto or desorption of molecules from the metal surface. Real-time changes in the SPR response can be measured using two different approaches: (a) SPR angle shift (Szabo *et al.* 1995; Hanken *et al.* 1996), the most commonly used method, in which the reflectivity of incident monochromatic light is monitored as a function of the incident angle (using instruments from BIACORE or Texas Instruments), and (b) SPR imaging (using instruments from GWC Technologies or HTS Biosystems), an array format technique that measures spatially resolved changes in reflectivity from a surface at a fixed angle and fixed wavelength (Brockman *et al.* 2000; Smith & Corn 2003). SPR imaging offers a distinct advantage over angle shift measurements as much larger numbers of biological interactions can be monitored simultaneously on a single surface compared to angle shift measurements.

A schematic diagram of the SPR imaging instrument used for the study of biomolecular interactions is shown in Fig. 1. Briefly, near infrared light from a collimated white light source is directed through a polarizer and is then incident on a high index glass prism optically coupled to a thin gold film to which probe molecules are attached. At a fixed angle the light interacts with the thin gold film patterned with biomolecules, creating surface plasmons and inducing an attenuation of the film reflectivity. Adsorption of molecules, such as nucleic acids or proteins onto the array elements results in changes in the reflectivity of the incident light, which are monitored with a CCD camera. Images with a minimum lateral resolution on the order of 50 μm can be achieved using an excitation wavelength of 830 nm. Samples can be injected onto the array surface through either a 100 μl flow cell or a polydimethylsiloxane (PDMS) microchannel with a total target solution volume of 1–10 μl.

Applications using SPR imaging include the detection and identification of DNA and RNA by hybridization adsorption onto DNA or RNA microarrays (Nelson *et al.* 2001; Lee *et al.* 2001; Goodrich *et al.* 2004*a*,*b*), protein–DNA binding using DNA arrays (Smith *et al.* 2003; Wegner *et al.* 2003; Kyo *et al.* 2004), antibody–antigen epitope mapping using peptide microarrays (Wegner *et al.* 2003), kinetic studies of enzymatic reactions of peptide microarrays (Wegner *et al.* 2004), and protein interactions using protein arrays (Kanda *et al.* 2004). SPR imaging measurements are quantitative and the change in percentage reflectivity ($\triangle\%R$) is directly proportional to the fractional surface binding coverage (θ), providing $\triangle\%R$ is below 10% (Nelson *et al.* 2001). The current sensitivity of the SPR imaging technique is about 10 fmol (10 μl of 10 nM solution) for 18-mer single-stranded DNA hybridized to a DNA array (Lee *et al.* 2001) and 1 fmol (10 μl of 1 nM solution) for specific antibody adsorption onto a peptide array (Wegner *et al.* 2002). Most recently Corn and colleagues (Goodrich *et al.* 2004*b*) demonstrated an enzymatically amplified SPR imaging method to detect 5 amol of 18-mer single-stranded DNA (500 μl of 10 fM solution) adsorbed onto an RNA array.

Label free detection provides a far greater degree of multiplexing compared to fluorescence based detection, which requires pairs of non-cross-reacting, high affinity antibody pairs (Peluso *et al.* 2003). SPR and related label-free detection platforms are also ideally suited for multiplexed analysis of association and dissociation rate constants for protein complexes, since all of the participants in the protein complex will yield an SPR imaging signal.

Surfaces for SPR analysis. A uniform presentation of surface immobilized proteins involves specific attachment to functionalized high density self-assembled monolayers (SAMs) prepared on planar gold surfaces. Most common protein array fabrication methods (Zhu *et al.* 2001; Haab *et al.* 2001) rely on the randomly orientated immobilization of proteins through amine or thiol groups present on the protein surface. In contrast, alkanethiol SAMs that are ω-terminated with a particular functional group provide a more robust and flexible platform for designing highly specific immobilization strategies (Frey & Corn, 1996; Frutos *et al.* 2000; Smith *et al.* 2001; Wegner *et al.* 2002, 2003; Sullivan & Huck, 2003) In this section, two different surface attachment procedures based on SATP (*N*-succinimidyl *S*-acetylthiopropionate) heterobifunctional cross-linking chemistry are discussed: (1) the use of SATP-DPDS (2,2′-dipyridyl disulphide) for thiol-containing biomolecules (i.e. cysteine terminated peptides; Smith *et al.* 2001; Wegner *et al.* 2002) and (2) the use of SATP-DTT (dithiothreitol) for His-tag proteins (Wegner *et al.* 2003). Both reaction schemes begin with a self-assembled monolayer of 11-mercapto-undecylamine

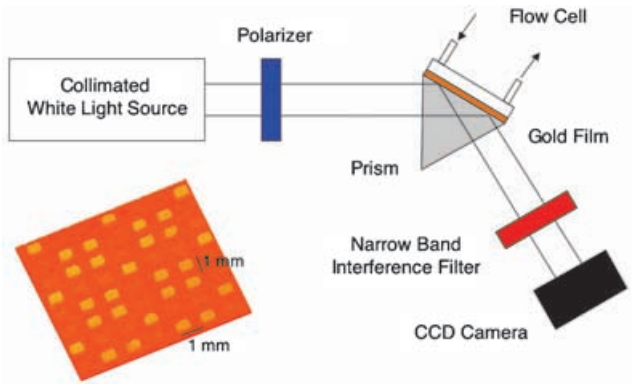

Figure 1. Schematic diagram of a SPR imaging set-up
An SPR difference image shown in the bottom-left corner of the figure was obtained for the sequence specific hybridization/adsorption of 18-mer target DNA onto a two component DNA array.

(MUAM) on a planar gold surface (45 nm thick). The MUAM surface is then reacted with SATP to create a reactive sulfhydryl-terminated surface. This involves a two step reaction: the NHS ester moiety of SATP reacts with the terminal amines of the packed monolayer forming a stable amide linkage and then a hydroxylamine solution containing DTT is used to remove the acetyl protecting group from the sulfhydryl revealing an active sulfhydryl surface. For thiol modified biomolecule attachment, this sulfhydryl surface is reacted with 2,2′-dipyridyl disulphide to form a pyridyl disulphide surface. Probe molecules such as cysteine terminated peptides and thiol modified DNA can then be immobilized to the surface via a thiol disulphide exchange reaction. A surface coverage of 10^{13} molecules cm^{-2} is typically attained. This approach has been successfully demonstrated with over 30 repeat hybridization–dehybridization cycles on a single DNA microarray (Smith *et al.* 2001). Moreover, this surface attachment chemistry has the additional advantage of being reversible; the disulphide bond can be cleaved in the presence of DTT to regenerate the sulfhydryl-terminated surface. In order to create a capture monolayer of His-tag proteins, the activated sulfhydryl surface is reacted with maleimide–nitrilotriacetic acid (NTA) forming a stable thioether linkage through the alkylation of the double bond of the maleimide.

The use of SAMs and heterobifunctional crosslinkers such as SATP can be adapted to fabricate microarrays containing individually addressable components useful for multiplexed detection. In one approach, UV photopatterning–deprotection chemistry is combined with either manual (Brockman *et al.* 1999; Nelson *et al.* 2001) or automatic spotters (Kyo *et al.* 2004) to attach over 150 different probe molecules on a 1.8 cm× 1.8 cm chip surface. Alternatively, PDMS microfluidic channels have been used with the specific aim of lowering detection limits, reducing analysis time and minimizing chemical consumption and sample volume (Lee *et al.* 2001). By changing the width and spacing of the PDMS microchannels, up to 100 individual array elements can be created (Lee *et al.* 2001).

Quantitative functional proteomics on protein chips: selective applications using label-free detection

Kinetic rate constants. SPR is ideally suited to measure the on- and off-rates of proteins and ligands from a surface bound proteome or subproteome. Most kinetic studies reported using SPR have been based on angle-shift measurements often restricted to one analyte assay per single substrate (O'Shannessy *et al.* 1993; Morton & Myszka, 1998; Suzuki *et al.* 2002; Chinowsky *et al.* 2003). However, time-resolved SPR measurements in an array format have been reported for the study of a streptavidin/biotin based system (Shumaker-Parry & Campbell, 2004; Shumaker-Parry *et al.* 2004). Additionally, kinetic values for transcription factor protein binding to double stranded DNA microarrays have been measured using real time SPR imaging (Kyo *et al.* 2004). Recent work by Corn and colleagues demonstrated multiplexed kinetic measurements of protein–peptide adsorption/desorption and surface enzymatic reactions (Wegner *et al.* 2004).

Figure 2*A* shows a representative kinetic curve obtained by monitoring the change in percentage reflectivity caused by the adsorption and desorption of S-protein onto an immobilized S-peptide microarray (Wegner *et al.* 2004). Upon introducing protein to the peptide array under continuous flow, an increase in signal is observed due to protein adsorption. The binding curve plateaus as a steady state is reached where protein adsorption and desorption rates are equal. Desorption of protein is observed when analyte-free buffer is flowed over the array surface. In order to extract values for the association (k_a) and dissociation (k_d) rate constants, sequential fitting of the response curves over a series of different protein concentrations is required. Based on a simple 1 : 1 interaction model between a protein analyte and a surface bound peptide molecule (i.e. A + B $\leftrightarrow$ AB), the rate of desorption of the complex AB can be described in terms of the SPR response ($\Delta\%R$):

$$\Delta\%R(t) = \Delta R\exp(-k_d t) \quad (1)$$

where ΔR is the maximum change in SPR signal measured at each protein concentration (O'Shannessy *et al.* 1993). For example, fitting a series of normalized S-protein desorption curves to eqn (1) yields a value for k_d of $1.0\ (\pm 0.08) \times 10^{-2}\ s^{-1}$. Importantly, the same slope was observed at different S-protein concentrations, indicating that the rate of desorption is independent of initial S-protein surface coverage. Figure 2*B* shows a series of adsorption curves obtained at different S-protein concentrations, which can be analysed using:

$$\Delta\%R(t) = \Delta R(1 - e^{-\gamma t}) \quad (2)$$

where $\gamma = k_a C + k_d$ with C being the protein concentration. ΔR can also be defined as equal to the product $\Delta R_{max}\theta$, where ΔR_{max} is the maximum SPR signal obtained when all surface binding sites are occupied and θ is the fraction of the total surface coverage. Therefore, a plot of γ *versus* C can be obtained such as that in Fig. 2*C* by fitting the adsorption curves shown in Fig. 2*B* to eqn (2). From the plot slope and intercept, respective values of $k_a = 1.9\ (\pm 0.05) \times 10^5\ M^{-1}\ s^{-1}$ and $k_d = 1.1\ (\pm 0.08) \times 10^{-2}\ s^{-1}$ can be obtained. The ratio of k_a and k_d defines the equilibrium adsorption constant (K_{Ads}) with a value of $1.7\ (\pm 0.1) \times 10^7\ M^{-1}$ for the S-protein and S-peptide interaction, which corresponds well with other independent equilibrium measurements (Connelly *et al.* 1990; Goldberg & Baldwin,

1999; Dwyer *et al.* 2001). This methodology was further utilized to simultaneously determine rate constants of S-protein adsorption/desorption onto multiple S-peptide derivatives in an array format using a single chip.

Protein interactions and activity. SPR imaging provides a powerful platform for surface based kinetic measurements of enzymatic reactions (Goodrich *et al.* 2004*a*) and enzymatic modification of proteins involving proteases (Wegner *et al.* 2004). During the last decade, peptide microarrays have been emerging as a promising tool for investigating enzymatic modifications of immobilized peptides (Mukhija *et al.* 1998; Wenschuh *et al.* 2000; Hilpert *et al.* 2001) by kinases, proteases and phophatases as well as identifying important residues in protein–protein recognition (Reineke *et al.* 1999; Reineke & Jerini, 2004, e.g. antibody–antigen epitope mapping). The most widespread array fabrication method used is based on SPOT technology, involving the combinatorial synthesis of peptide libraries on a cellulose membrane at discrete locations (Mukhija *et al.* 1998; Reineke *et al.* 2001, 2004). The majority of peptide microarray based assays employ fluorescent, enzymatic or radioactive detection. SPR is an ideal solution when labelling is difficult and can interfere with the biological activity of the target molecule. Unlike SPOT technology, SPR imaging detection is based on the use of specifically developed surface chemistry (see Surfaces for SPR analysis) for the controlled attachment of biomolecular probes.

Multiplexed epitope mapping and analysis of protease and kinase substrate specificity. In this section, the use of peptide microarrays for the study of FLAG antibody epitope mapping and the sequence specific factor Xa cleavage reaction using SPR imaging is described as an example of how SPR imaging can be used to determine protein activity and specificity. In both cases, patterned peptide arrays were created using a set of parallel PDMS microchannels (Wegner *et al.* 2002, 2004). A second microchannel with a serpentine design was used as a small volume flow cell (5 μl) to introduce target solutions to the peptide surface. Figure 3*A* (from Wegner *et al.* 2002) shows differential binding of anti-FLAG M2 to a peptide array composed of four different peptide epitopes, selected from the critical residues of the FLAG binding motif (Slootstra *et al.* 1996). The highest SPR signal was observed for F1, the original peptide, while F2 and F3, which contained alanine substitutions for amino acids in the binding motif, showed the least anti-FLAG adsorption. As well as distinguishing between peptide sequences differing by a single amino acid substitution, quantitative analysis of the SPR images at different anti-FLAG concentrations yielded values for the adsorption coefficient (K_{Ads}), for

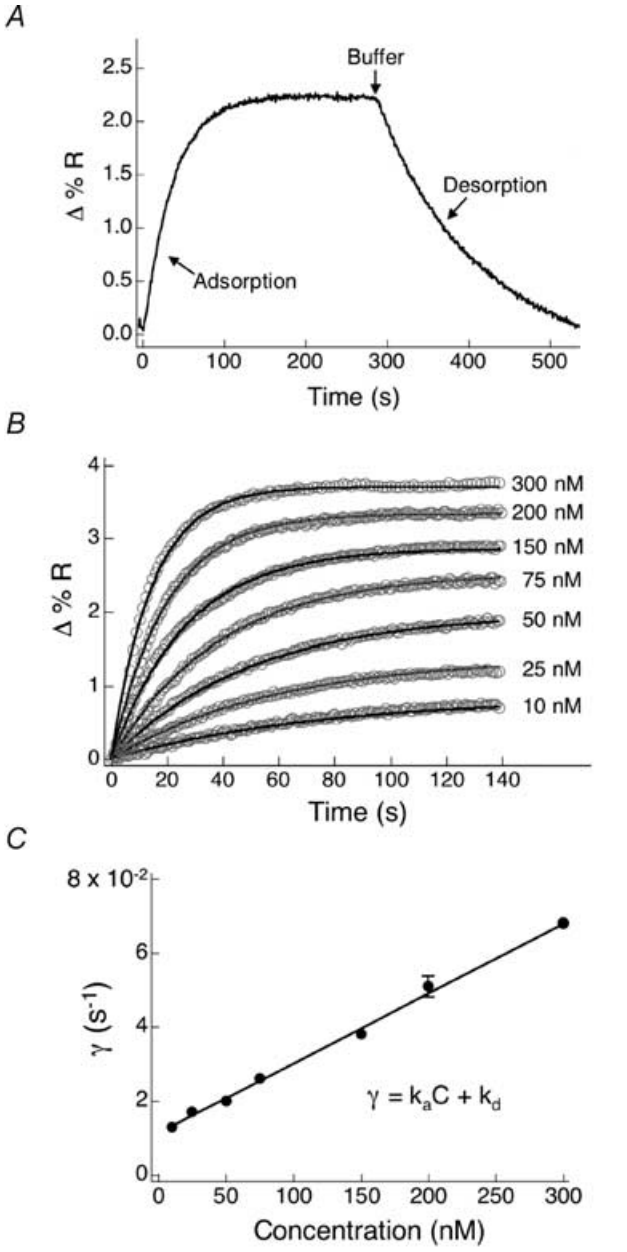

Figure 2. Quantitative analysis of the adsorption/desorption kinetics of S protein onto an S peptide microarray using real–time SPR imaging
A, a plot representing $\triangle\%R$ as a function of time for the sequential adsorption and desorption of S-protein onto an S-peptide microarray. Using neighbouring control array elements, the plot was background corrected for experimental factors such as non-specific binding and bulk refractive index changes. *B*, a series of adsorption curves obtained for various concentrations of S-protein onto an S-peptide array surface. *C*, a plot of gamma values *versus* S-protein concentration obtained from fitting the adsorption curves in Fig. 2*B*. The linear slope is equal to the adsorption rate constant (k_a), and the *y*-intercept corresponds to the desorption rate constant (k_d). Reproduced with permission from Wegner *et al.* (2004), *Analytical Chemistry* **76**, 5677–5684; © 2004 American Chemical Society.

the different peptide interactions, which were comparable to solution measurements of equilibrium dissociation constants.

Peptide microarrays used in conjunction with SPR imaging have been used to study the enzymatic reaction of factor Xa protease. Understanding the intricacies of factor Xa cleavage is of importance due to its role in the regulation of the clotting cascade and in haemophilia clinical assays (Rai *et al.* 2001; Bianchini *et al.* 2002). As an example, Fig. 3*B* (from Wegner *et al.* 2004) demonstrates real-time monitoring of the differential proteolytic cleavage of multiple peptide array elements by Xa. These peptide array elements contained the wild-type recognition substrate, a mutant substrate, and a negative control peptide sequence. From the real time data, the reaction rates of Xa cleavage on both the wild-type and mutant peptide sequence were obtained. The wild-type substrate was shown to undergo proteolytic cleavage 10 times faster than the mutant substrate (Wegner *et al.* 2004).

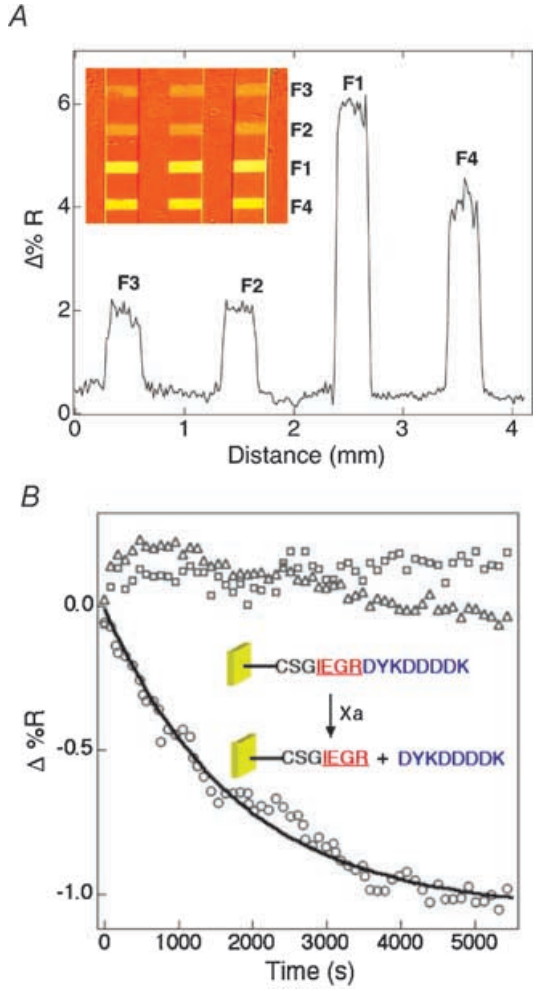

Figure 3. SPR imaging measurements of multiplexed epitope mapping and protease substrate specificity
A, an SPR difference image showing the binding of 100 nM solution of anti-FLAG M2 to a peptide array composed of F1, F2, F3 and F4. F1: original FLAG sequence (CSGDYKDDDDK); F2 and F3: alanine substitutions for the residue 2 tyrosine and residue 3 lysine, respectively; and F4: alanine substitution for residue 5 aspartic acid, which was not identified as part of the binding motif. The line profile shows the differential binding of antibody to the multicomponent peptide array. *B*, plot representing the differential proteolytic cleavage reaction of a three component peptide array composed of wild-type substrate (○), mutant substrate (△) and FLAG peptide control (□). Inset shows the removal of FLAG peptide portion from the substrate sequence by factor Xa. Reproduced with permission from Wegner *et al*. (2002), *Analytical Chemistry*74, 5161–5168; © 2002 American Chemical Society; and Wegner *et al.* (2004), *Analytical Chemistry* **76**, 5677–5684; © 2004 American Chemical Society.

In addition to protease studies using peptide microarrays, a protein chip that contains an array of 97.5% of the known protein kinases in yeast has been described by Zhu *et al.* (2000). This was used for multiplexed functional proteomic analysis to quantify their activities and determine substrate specificities. The kinases were expressed as GST-fusions in *E. coli* and purified using a glutathione affinity matrix. The authors isolated 119 soluble protein kinases, which were covalently attached to the surface of 300 nl silicon microwells through the immobilized thiol reactive crosslinker (Zhu *et al.* 2000). Protein kinase activities were determined for 17 different kinase substrates within the array by measuring the rate of ^{32}P incorporation from ATP into tyrosine kinase substrates. The authors used these chips for multiplexed, high throughput functional proteomic analysis of protein kinase activity including analyses of substrate specificity that provided new information on key amino acids found in the vicinity of the catalytic active site of tyrosine kinases. The availability of protein kinase chips and knowledge of their substrate specificities should greatly facilitate the discovery of specific inhibitors within chemical libraries that may prove useful in treating various diseases.

Fluorescence based analysis of conformational dynamics in functional protein complexes

A complete functional analysis of a proteome or subproteome should include a study of the mechanisms that underlie protein function. These studies are essential to our understanding of complex cellular processes such as muscle contraction and cell motility. For example, while the protein components of the cardiac thin filament complex have been known for more than four decades, the mechanism underlying the regulation of thin filament activation is still controversial (Huxley, 1972; Squire & Morris, 1999; Xu *et al.* 1999). The Marriott laboratory has developed an approach to map protein motions within actomyosin and cardiac thin filaments that uses FRET techniques to measure changes in the proximity between specific sites on actin and thin filament proteins at the level of single filaments sliding on myosin (Heidecker *et al.* 1995; Yan & Marriott, 2003*b*). While

FRET based measurements of distance are less precise than those obtained from X-ray crystallography, this approach has the advantage of generating information on functional motions within large molecular complexes at physiologically relevant concentrations and within physiologically relevant solutions. Microscope based functional and mechanistic analyses of other protein machines have been described including the multiprotein, actin nucleation complex Arp2/3-WASP/Scar (Blanchoin *et al.* 2000), the Fo-ATPase (Kinosita *et al.* 2004), RNA polymerase (Harada *et al.* 1999), and the microtubule–kinesin motor protein complex (Friedman & Vale, 1999).

Conformational dynamics in functional actomyosin filament complexes

Kron & Spudich (1986) developed a surface based motility assay to analyse interactions and activities between single actin filaments and myosin on the chip surface – the assay provides a truly functional assessment of the actomyosin complex because it measures how well the free energy associated with the binding and hydrolysis of ATP and release of hydrolysis products within the complex is coupled to the movement of actin filaments – the measured sliding velocity of single filaments at $5\,\mu m\,s^{-1}$ is close to the unloaded sliding velocity in skeletal muscle (Kron & Spudich, 1986). The motility assay can therefore be used to study structure–function relationships at the level of a single actin filaments interacting with only a few myosin molecules. Further modifications to the assay (Gordon *et al.* 1997; Gerson *et al.* 1999) make it possible to analyse the role of structural dynamics for specific thin filament proteins, e.g. troponin C and tropomyosin, and calcium ions, in regulating the contraction of single cardiac thin filaments. Finally this system can also be used to investigate the effects of specific mutations in tropomyosin and troponin subunits (e.g. those found in hypertrophic cardiomyopathies) on the sliding velocity and Ca^{2+} sensitivity of thin filament function (Bing *et al.* 2000).

The Marriott lab has modified the motility assay for high resolution, fluorescence imaging microscopy based spectroscopic analyses of functional protein motions within actin and thin filament proteins (Fig. 4) – the goal for these studies is to correlate structural dynamics of actin, thin filament proteins and myosin to specific steps in the regulation and contraction of actin filaments. For example, fluorescence imaging of single actin filaments has been used to investigate the role if any of protein motions within actin and functional thin filaments as they move on myosin (Heidecker *et al.* 1995). In these studies single actin filaments were stoichiometrically labelled with FITC–phalloidin and TRITC–phalloidin – these probes serve to visualize individual actin filaments as they move on the myosin coated surface, and to map changes in probe orientation (fluorescence polarization) and molecular proximity (FRET) between the phalloidin binding sites on filaments as they slide on myosin (Fig. 5; Heidecker *et al.* 1995; Yan & Marriott, 2003*a*). In Fig. 5*B* and *C* we show an image field containing three different types of labelled actin filaments bound with either the donor probe (D), the donor and acceptor probes (D/A; Fig. 5*B*) and acceptor probe (A; Fig. 5*C*). Steady state fluorescence imaging of filaments in an image field using donor excitation (488 nm) and donor emission (520 nm) reveals two of the three filament types (D and D/A; Fig. 5*B*). The D/A and A only containing filaments are identified using 546 nm excitation and 580 nm emission (Fig. 5*C*). Quantitative analysis of FRET within the D/A

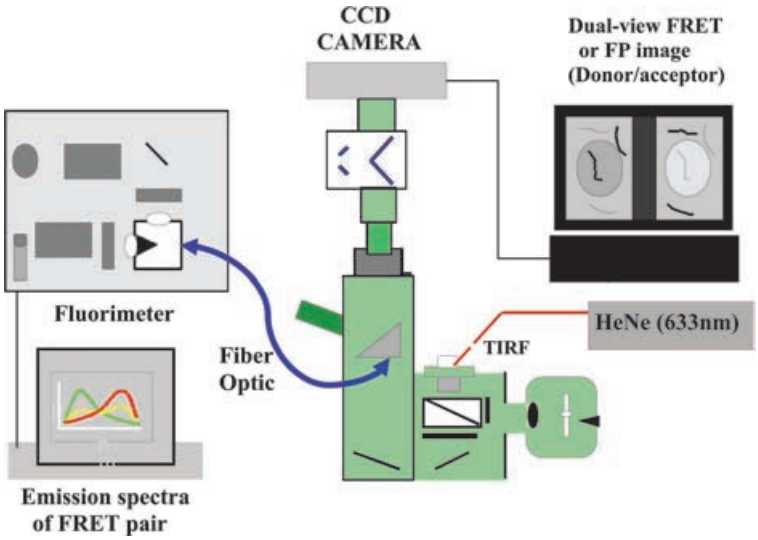

Figure 4. FRET and FP imaging microscope for measurements of FRET and fluorescence polarization on single actin filaments
The fluorescence emission from the surface bound protein complex excited by conventional epi- or total internal reflection (TIRF) illumination can be directed to a fluorometer via a fibre optic to record the fluorescence emission spectra or else directed through a double-view adaptor, which separates the donor and sensitized emission (or polarized components of the emission) using a pair of dichroic mirrors before being detected by the CCD camera.

filaments is performed by measuring the intensities of donor fluorescence along the length of D/A and D filaments in the same image field (Fig. 5*B*). FRET efficiency is calculated following corrections for the number of donor probes within each filament, the random distribution and local background signal according to Heidecker *et al.* (1995). These quantitative fluorescence-imaging studies show that the phalloidin probe is fixed on the actin filament and does not undergo any significant motions while the filament slides on myosin. FRET between the D and A probes is shown to occur between adjacent actin protomers (N and $N+1$; $R = 3.8$ nm) rather than between actin protomers along the same long-pitched actin helix (N and $N+2$; 5.5 nm; Heidecker *et al.* 1995). This experimental system can also be used to determine whether the phalloidin probe and, by implication, the actin protomer experience rotational motions during sliding on myosin. Thus steady state fluorescence polarization image microscopy (FPIM) of single actin filaments labelled with tetramethylrhodamine (TMR)–phalloidin (Fig. 5*D* and *E*) shows that the TMR probe is highly immobilized and orientated at an angle of ~30 deg with respect to the filament axis on the filament and does not undergo any significant rotational motion while sliding on myosin (Yan & Marriott, 2003*a*). These studies suggest that the actin protomers in a filament play a rather passive role in the contraction of actomyosin. On the other hand, we expect that the same FRET/FPIM approach applied to fluorescently troponin subunits and tropomyosin within thin filaments will reveal more dramatic structural dynamics that are proposed to underlie the regulation of muscle contraction (Huxley, 1972; Xu *et al.* 1999).

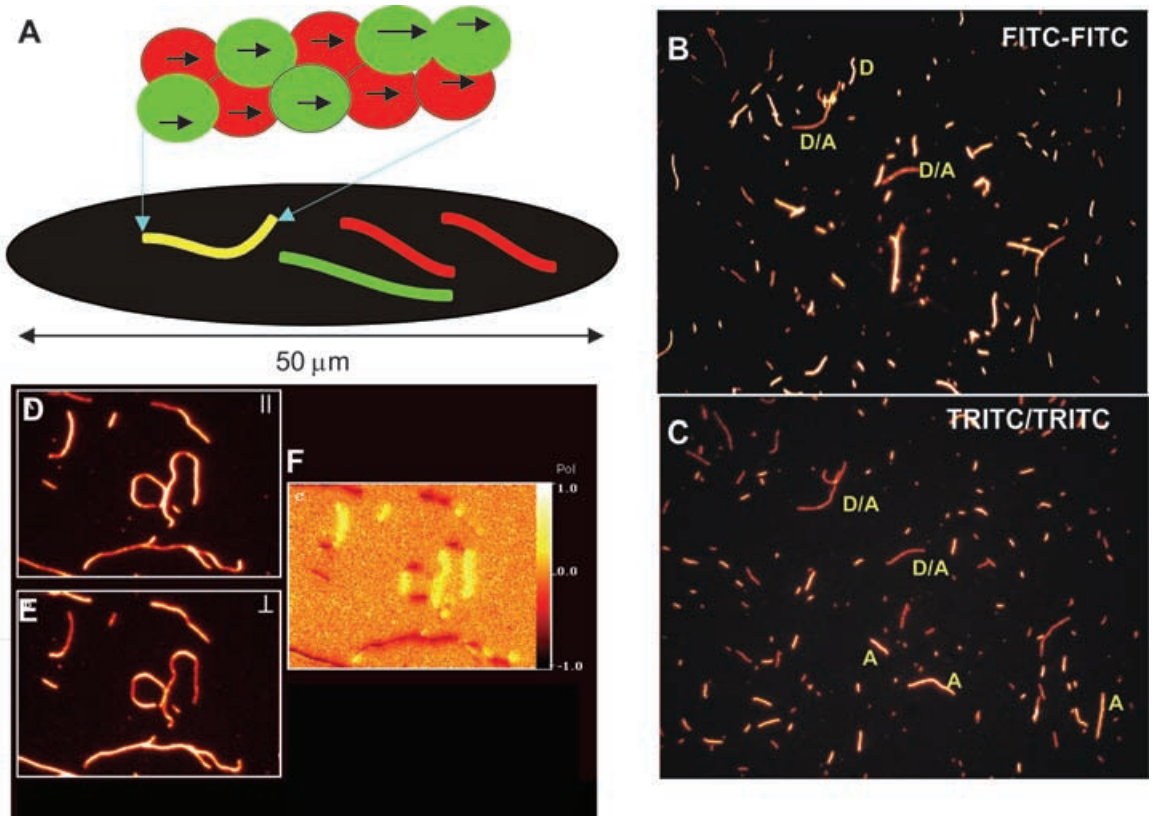

Figure 5. Surface based determinations of molecular proximity and orientation within single actin filament complexes

A, schematic representation of the actomyosin motility assay. Single actin filaments harbouring donor and acceptor probes at specific sites on each protomer are laid down on a monolayer of myosin and visualized using the microscope described in Fig. 4. *B* and *C*, three types of filaments (donor only (D), donor–acceptor (D/A) and acceptor only (A)) are bound to myosin. The addition of 1 mM ATP results in the motility of filaments at 5 μm s^{-1}. FRET efficiency is determined for filaments in the absence and presence of ATP by comparing emission intensities of the donor only and donor–acceptor filaments (Fig. 5*B*) according to Heidecker *et al.* (1995). *D* and *E*, polarizing beam splitters are used in the double view adaptor for FP based imaging of molecular orientation on single actin filaments. *F*, the value of the corrected polarization for TRITC–phalloidin molecules is computed on a pixel by pixel basis for each actin filament in the field.

Summary

The combination of SPR imaging measurements and quantitative fluorescence microscopy of protein and peptide microarrays exhibits great potential in multiplexed functional proteomic analysis of protein interactions. We have also highlighted in this article how quantitative fluorescence microscopy can be used to understand the mechanism of protein-driven reactions by correlating specific motions within protein machines to function. These two techniques should prove to be invaluable tools for the quantitative, kinetic analysis of protein binding reactions and protein activity as well as the characterization and kinetic analysis of post-translational modifications of proteins. These two approaches are also suitable in translational research including high throughput screening of drugs that inhibit specific enzymatic activities involving kinases, proteases and phosphatases.

References

Aebersold R & Mann M (2003). Mass spectrometry-based proteomics. *Nature* **422**, 198–207.

Bianchini EP, Louvain VB, Marque PE, Juliano MA, Juliano L & Le Bonniec BF (2002). Mapping the catalytic groove preferences of factor Xa reveals an inadequate selectivity for its macromolecule substrates. *J Biol Chem* **277**, 20527–20534.

Bing W, Knott A, Redwood C, Esposito G, Purcell I, Watkins H & Marston S (2000). Effect of hypertrophic cardiomyopathy mutations in human cardiac muscle alpha-tropomyosin (Asp175Asn and Glu180Gly) on the regulatory properties of human cardiac troponin determined by in vitro motility assay. *J Mol Cell Cardiol* **32**, 1489–1498.

Blanchoin L, Amann KJ, Higgs HN, Marchand JB, Kaiser DA & Pollard TD (2000). Direct observation of dendritic actin filament networks nucleated by Arp2/3 complex and WASP/Scar proteins. *Nature* **404**, 1007–1011.

Brockman JM, Frutos AG & Corn RM (1999). A multistep chemical modification procedure to create DNA arrays on gold surfaces for the study of protein–DNA interactions with surface plasmon resonance imaging. *J Am Chem Soc* **121**, 8044–8051.

Brockman JM, Nelson BP & Corn RM (2000). Surface plasmon resonance imaging measurements of ultra organic films. *Annu Rev Phys Chem* **51**, 41–63.

Chen GY, Uttamchandani M, Zhu Q, Wang G & Yao SQ (2003). Developing a strategy for activity-based detection of enzymes in a protein microarray. *Chembiochem* **4**, 336–339.

Chinowsky TM, Quinn JG, Bartholomew DU, Kaiser R & Elkind JL (2003). Performance of the Spreeta 2000 integrated surface plasmon resonance affintiy sensor. *Sens Act B* **91**, 266–274.

Choidas A, Jungbluth A, Sechi A, Ullrich A & Marriott G (1998). The suitability and application of a GFP-actin fusion protein for long-term imaging of the organization and dynamics of the cytoskeleton in mammalian cells. *Eur J Cell Biol* **77**, 81–90.

Connelly PR, Varadarajan R, Sturtevant JM & Richards FM (1990). Thermodynamics of protein-peptide interactions in the Ribonuclease S system studied by titration calorimetry. *Biochem* **29**, 6108–6114.

Dwyer JJ, Dwyer MA & Kossiakoff AA (2001). High affinity S-peptide variants obtained by phage display have a novel 'hot-spot' of binding energy. *Biochem* **40**, 13941–13500.

Frey BL & Corn RM (1996). Covalent attachment and derivitization of poly (L-lysine) monolayers on gold surfaces as characterized by polarization-modulation FT-IR spectroscopy. *Anal Chem* **68**, 3187–3193.

Friedman DS & Vale RD (1999). Single molecule analysis of kinesin motility reveals regulation by the cargo-binding tail domain. *Nature Cell Biol* **1**, 293–297.

Frutos AG, Brockman JM & Corn RM (2000). Reversible protection and reactive patterning of amine- and hydroxyl-terminated self-assembled monolayers on gold surfaces for the fabrication of biopolymer arrays. *Langmuir* **16**, 2192–2197.

Gerson JH, Bobkova E, Homsher E & Reisler E (1999). Role of residues 311/312 in actin–tropomyosin interaction. In vitro motility study using yeast actin mutant e311a/r312a. *J Biol Chem* **274**, 17545–17550.

Goldberg JM & Baldwin RL (1999). A specific transition state for S-peptide combining with folded S-protein and then refolding. *Proc Natl Acad Sci U S A* **96**, 2019–2024.

Goodrich TT, Lee HJ & Corn RM (2004*a*). Direct detection of genomic DNA by enzymatically amplified SPR imaging measurements of RNA microarrays. *J Am Chem Soc* **126**, 4086–4087.

Goodrich TT, Lee HJ & Corn RM (2004*b*). Enzymatically amplified surface plasmon resonance imaging method using RNase H and RNA microarrays for the ultrasensitive detection of nucleic acids. *Anal Chem* **76**, 6173–6178.

Gordon AM, LaMadrid MA, Chen Y, Luo Z & Chase PB (1997). Calcium regulation of skeletal muscle thin filament motility in vitro. *Biophys J* **72**, 1295–1307.

Graves PR & Haystead TAJ (2003). A Functional proteomics approach to signal transduction. *Recent Prog Hormone Res* **58**, 1–24.

Gygi S, Rochon Y, Fransz B & Aebersold R (1999). Correlation between protein and mRNA abundance in yeast. *Mol Cell Biol* **19**, 1720–1730.

Haab BB, Dunham MJ & Brown PO (2001). Protein microarrays for highly parallel detection and quantitation of specific proteins and antibodies in complex solutions. *Genome Biol* **2**, 1–13.

Hanken DG, Jordan CE, Frey BL & Corn RM (1996). Surface plasmon resonance measurements of ultrathin organic films at electrode surfaces. In *Electroanalytical Chemistry*, vol 20, ed. Bard AJ & Rubinstein I, pp. 141–225. Marcel Dekker, New York.

Harada Y, Funatsu T, Murakami K, Nonoyama Y, Ishihama A & Yanagida T (1999). Single-molecule imaging of RNA polymerase–DNA interactions in real time. *Biophys J* **76**, 709–715.

Heidecker M, Yan-Marriott Y & Marriott G (1995). Proximity relationships and structural dynamics of the phalloidin binding site of actin filaments in solution and on single actin filaments on heavy meromyosin. *Biochemistry* **34**, 11017–11025.

Hilpert K, Hansen G, Wessner H, Kuttner G, Wefle K, Seifert M & Hohne W (2001). Anti-c-myc 9E10: epitope key positions and variability characterized using peptide spot synthesis on cellulose. *Prot Eng* **14**, 803–806.

Homola J, Yee SS & Gauglitz G (1999). Surface plasmon resonance sensors (review). *Sens Actuators B* **54**, 3–15.

Huxley HE (1972). Structural changes in the actin and myosin-containing filaments during contraction. *Cold Spring Harbor Symposium Quant Biol* **37**, 361–376.

Kanda V, Kariuki JK, Harrison DJ & McDermott MT (2004). Label-free reading of microarray-based immunoassays with surface plasmon resonance imaging. *Anal Chem* **76**, 7257–7262.

Kinosita K Jr, Adachi K & Itoh H (2004). Rotation of F1-ATPase: how an ATP-driven molecular machine may work. *Annu Rev Biophys Biomol Struct* **33**, 245–268.

Kron J & Spudich JA (1986). Fluorescent actin filaments move on myosin fixed to a glass surface. *Proc Natl Acad Sci U S A* **83**, 6272–6276.

Kyo M, Yamamoto T, Motohashi H, Kamiya T, Kuroita T, Tanaka T, Engel JD, Kawakami B & Yamamoto M (2004). Evaluation of MafG interaction with Maf recognition element arrays by surface plasmon resonance imaging technique. *Genes Cells* **9**, 153–164.

Lee HJ, Goodrich TT & Corn RM (2001). SPR imaging measurements of 1-D and 2-D DNA microarrays created from microfluidic channels on gold thin films. *Anal Chem* **73**, 5525–5531.

MacBeath G & Schreiber SL (2000). Printing proteins as microarrays for high-throughput function determination. *Science* **289**, 1760–1763.

Morton TA & Myszka DG (1998). Kinetic analysis of macromolecular interactions using surface plasmon resonance biosensors. *Meth Enzymol* **295**, 268–295.

Mukhija S, Germeroth L, Schneider-Mergener J & Erni B (1998). Identification of peptides inhibiting enzyme I of the bacterial phosphotransferase system using combinatorial cellulose-bound peptide libraries. *European J Biochem* **254**, 433–438.

Murakoshi H, Iino R, Kobayashi T, Fujiwara T, Ohshima C, Yoshimura A & Kusumi A (2004). Single-molecule imaging analysis of Ras activation in living cells. *Proc Natl Acad Sci U S A* **101**, 7317–7322.

Nelson BP, Grimsrud TE, Liles MR, Goodman RM & Corn RM (2001). Surface plasmon resonance imaging measrements of DNA and RNA hybridization adsorption onto DNA microarrays. *Anal Chem* **73**, 1–7.

O'Shannessy DJ, Brigham-Burke, Soneson KK, Hensley P & Brooks I (1993). Determination of rate and equlibrium binding constants for macromolecular interactions using surface plasmon resonance: use of nonlinear least squares analysis methods. *Anal Biochem* **212**, 457–468.

Peluso P, Wilson DS, Do D, Tran H, Venkatasubbaiah M, Quincy D, Heidecker B, Poindexter K, Tolani N, Phelan M *et al.* (2003). Optimizing antibody immobilization strategies for the construction of protein microarrays. *Anal Biochem* **312**, 113–124.

Ping P-P (2003). Identification of novel signaling complexes by functional proteomics. *Circulation Res* **93**, 595–603.

Pjizicky E, Bastiaens PIH, Zhu H, Snyder M & Field S (2003). Protein analysis on a proteomic scale. *Nature* **422**, 208–215.

Pollard TD & Borisy GG (2003). Cellular motility driven by assembly and disassembly of actin filaments. *Cell* **113**, 549.

Rai R, Sprengeler PA, Elrod KC & Young WB (2001). Perspectives on factor Xa inhibition. *Curr Med Chem* **8**, 101–119.

Reineke U & Jerini AG (2004). Antibody epitope mapping using arrays of synthetic peptides. *Meth Mol Biol* **248**, 443–463.

Reineke U, Kramer A & Schneider-Mergener J (1999). Antigen sequence- and library-based mapping of linear and discontinuous protein–protein interaction sites by SPOT synthesis. *Cur Top, Microbiol Immunol* **243**, 23–36.

Reineke U, Volkmer-Engert R & Schneider-Mergener J (2001). Applications of peptide arrays prepared by the SPOT-technology. *Current Opinion Biotechnol* **12**, 59–64.

Resing KA (2002). Analysis of signaling pathways using functional proteomics. *Ann New York Acad Sci* **971**, 608–614.

Roy P, Rajfur Z, Jones D, Marriott G, Loew L & Jacobson K (2001). Local photorelease of caged thymosin β4 in locomoting keratocytes causes cell turning. *J Cell Biol* **153**, 1035–1047.

Shumaker-Parry JS & Campbell CT (2004). Quantitative methods for spatially resolved adsorption/desorption measurements in real time by surface plasmon resonance microscopy. *Anal Chem* **76**, 907–917.

Shumaker-Parry JS, Zareie MH, Aebersold R & Campbell CT (2004). Microspotting streptavidin and double stranded DNA arrays on gold for high-throughput studies of protein–DNA interactions by surface plasmon resonance microscopy. *Anal Chem* **76**, 918–929.

Slootstra JW, Kuperus D, Pluckthun A & Meloen RH (1996). Identification of new tag sequences with differential and selective recognization properties for the anti-FLAG monoclonal antibodies M1, M2, and M5. *Mol Divers* **2**, 156–164.

Smith EA & Corn RM (2003). Surface plasmon resonance imaging as a tool to monitor biomolecular interactions in an array based format. *Appl Spect* **57**, 320A–332A.

Smith EA, Erickson MG, Ulijasz AT, Weisblum B & Corn RM (2003). Surface plasmon resonance imaging of transcription factor proteins: Interactions of bacterial response regulators with DNA arrays on gold films. *Langmuir* **19**, 1486–1492.

Smith EA, Wanat MJ, Cheng Y, Barreira SVP, Frutos AG & Corn RM (2001). Formation, spectroscopic characterization, and applications of sulfhydryl-terminated alkanethiol monolayers for the chemical attachment of DNA onto gold surfaces. *Langmuir* **17**, 2502–2507.

Squire JM & Morris EP (1999). A new look at filament regulation in vertebrate skeletal muscle. *FASEB J* **12**, 760–771.

Sullivan TP & Huck WTS (2003). Reactions on monolayers: Organic synthesis in two dimensions. *Eur J Org Chem* **2003**, 17–29.

Suzuki M, Ozawa F, Sugimoto W & Aso S (2002). Miniature surface plasmon resonance immunosensors-rapid and repetitive procedure. *Anal Bioanal Chem* **372**, 301–304.

Szabo A, Stolz L & Granzow R (1995). Surface plasmon resonance and its use in biomolecular interaction analysis (BIA). *Curr Opin Struct Biol* **5**, 699–705.

Wegner GJ, Lee HJ & Corn RM (2002). Characterization and optimization of peptide arrays for the study of epitope–antibody interactions using surface plasmon resonance imaging. *Anal Chem* **74**, 5161–5168.

Wegner GJ, Lee HJ, Marriott G & Corn RM (2003). Fabrication of histidine-tagged fusion protein arrays for surface plasmon resonance imaging studies of protein-protein and protein–DNA interactions. *Anal Chem* **75**, 4740–4746.

Wegner GJ, Wark AW, Lee HJ, Codner E, Saeki T, Fang S & Corn RM (2004). Real-time SPR imaging measurements for the multiplexed determination of protein adsorption/desorption kinetics and surface enzymatic reactions on peptide microarrays. *Anal Chem* **76**, 5677–5684.

Wenschuh H, Volkmer-Engert R, Schmidt M, Schulz M, Schneider-Mergener J & Reineke U (2000). Coherent membrane supports for parallel microsynthesis and screening of bioactive peptides. *Biopolymers* **55**, 188–206.

Xu C, Craig R, Tobacman L, Horowitz R & Lehman W (1999). Tropomyosin positions in regulated thin filaments revealed by cryoelectron microscopy. *Biophys J* **77**, 985–992.

Yan Y & Marriott G (2003*a*). Fluorescence resonance energy transfer imaging microscopy and fluorescence polarization imaging microscopy. *Meth Enzymol* **360**, 561–580.

Yan Y & Marriott G (2003*b*). Analysis of protein interactions using fluorescence technologies. *Curr Opin Chem Biol* **7**, 635–640.

Zhu H, Bilgin M, Bangham R, Hall D, Casamayor A, Bertone P, Lan N, Jansen R, Bidlingmaier S, Houfek T, Mitchell T, Miller P, Dean RA, Gerstein M & Snyder M (2001). Global analysis of protein activities using proteome chips. *Science* **293**, 2101–2105.

Zhu H, Klemic JF, Chang S, Bertone P, Casamayor A, Klemic KG, Smith D, Gerstein M, Reed MA & Snyder M (2000). Analysis of yeast protein kinases using protein chips. *Nature Genet* **26**, 283–289.

Zhu H & Snyder M (2003). Protein chip technology. *Curr Opin Chem Biol* **7**, 55–63.